An Efficient Method to Capture the Impact of Total Knee Replacement on a Variety of Simulated Patient Types: A Finite Element Study

Medical Engineering and Physics 38 (2016) 959–968

Contents lists available at ScienceDirect

Medical Engineering and Physics

journal homepage: www.elsevier.com/locate/medengphy

An efficient method to capture the impact of total knee replacement on a variety of simulated patient types: A finite element study

Noel Conlisk[a,b,*], Colin R. Howie[c], Pankaj Pankaj[b]

[a] School of Clinical Sciences, The University of Edinburgh, Edinburgh, UK
[b] School of Engineering, The University of Edinburgh, Edinburgh, UK
[c] Department of Orthopaedics, New Royal Infirmary of Edinburgh, Old Dalkeith Road, Little France, Edinburgh, UK

ARTICLE INFO

Article history:
Received 16 January 2016
Revised 8 April 2016
Accepted 8 June 2016

Keywords:
Total knee arthroplasty
Variable properties
Finite element analysis
Young vs. old
osteoporosis

ABSTRACT

Osteoporosis resulting in a reduction in bone stiffness and thinning of the cortex is almost universal in older patients. In this study a novel method to generate computational models of the distal femur which incorporate the effects of ageing and endosteal trabecularisation are presented. Application of this method to pre- and post-knee arthroplasty scenarios is then considered. These computational methods are found to provide a simple yet effective tool for assessing the post-arthroplasty mechanical environment in the knee for different patient types and can help evaluate vulnerability to supracondylar periprosthetic fracture following implantation. Our results show that the stresses in the periprosthetic region increase dramatically with ageing; this is particularly true for higher flexion angles. Stresses in the anterior region of the femoral cortex were also found to increase significantly post-implantation. The most dramatic increases in stresses and strains at these locations were observed in old osteoporotic patients, explaining why this patient group in particular is at greater risk of periprosthetic fractures.

1. Introduction

Ageing and osteoporosis both lead to deterioration in bone quality. Due to medical advances the global population as a whole is ageing. Therefore, consideration of how the change in bone quality influences the mechanical environment of the femur after total knee arthroplasty (TKA) assumes great importance, particularly since the number of operations performed each year continues to increase [1]. In general, TKA is a successful operation with implant survival rates at 10–15 years of greater than 90% [2,3]. However, a number of studies have shown the potential for failure or complication arising post-implantation, leading to an increase in the number of revision surgeries performed [4–6]. These studies have also shown that the incidence of periprosthetic supracondylar fracture increases over time, probably due to a combination of "physiological" and periprosthetic osteoporosis. At the time of revision surgery the quality of bone for fixation is important in terms of the stability of the replacement revision prosthesis and hence its longevity. Areas immediately under the primary implants, particularly behind the anterior flange and posterior condyles of the femur develop significant periprosthetic osteoporosis [7–10]. Bone loss under the implant and stress concentrations around the implant are thought to influence the pattern of periprosthetic femoral fracture [6,8,11].

The use of finite element (FE) models as a tool to investigate complex clinical scenarios and critical cases is becoming more widely accepted. These models provide information which cannot easily be obtained from a lab or clinical research investigation. Studies often use CT based inhomogeneous material properties for the bone [12–14] in which the variation of elastic modulus is estimated from the variation of apparent bone density in the specific femur being considered. Few studies in the literature directly compare the influence of healthy and osteoporotic bone on the femur [15–17] due to this specificity, fewer still have investigated the influence of bone properties following joint arthroplasty on the mechanical environment in the femur e.g. [18,19].

In a study of 163 patients, Bousson et al. [20] employed microradiographs and image analysis techniques to investigate the influence of age and gender on the porosity of three sub-regions (endosteal, mid-cortical and periosteal) from the anterior cortex of the femoral mid-shaft. The authors found that pore size and number increased with increasing age in younger patients (< 60 years). Furthermore, it was observed that pore size and number were proportionally similar in each of the three sub-regions in male specimens, whereas female specimens exhibited significant

* Corresponding author at: The Queen's Medical Research Institute, 47 Little France Crescent, The University of Edinburgh, EH16 4TJ Edinburgh, UK. Tel.: +44 131 242 9219.
E-mail address: noel.conlisk@ed.ac.uk, noecon@gmail.com (N. Conlisk).

http://dx.doi.org/10.1016/j.medengphy.2016.06.014
1350-4533/

cortical thinning in the endosteal sub-region in particular. Similarly, a more recent study of 688 women and 561 men by Russo et al. [21] indicated that cortical thickness in female specimens of 80 years or greater is approximately 50% of that measured in younger female samples. Age related variations to the bone geometry and porosity at the microscopic [20,22] and macroscopic levels [21] can have considerable impact on its mechanical properties and may have serious implications for fracture risk. The majority of previous research has focused on modeling cases representing a normal patient. It has been well documented that as we age our bones undergo mechanical and structural changes [20–22]. As a result implants designed to suit an average and otherwise healthy patient may induce a very different response in an elderly or pathological patient.

In the present study, FE models of the intact and post-TKA (employing posterior stabilising or PS implant) distal femur were developed. The aim of this study was to determine how incorporation of the effects of ageing (by means of a reduction in bone stiffness) and trabecularisation (modelled through pseudo-thinning) of the cortex, influence the observed mechanics post-implantation.

2. Methods

A three-dimensional virtual reconstruction [23] of the large left fourth generation composite femur (Sawbones; Pacific Research Laboratories, Vashon, Washington, USA), was used for this study (Fig. 1). This geometry was subsequently modified to accept the posterior stabilising (PS) implant, also shown in Fig. 1. Physical implant measurements and surgical theatre templates were used in conjunction with computer aided design software (Autodesk Inventor 2010, Autodesk Inc. San Rafael, California, U.S) to develop 3D models of the femoral implant; the same software was also used to incorporate surgical cuts into the femur for accommodating a posterior stabilizing (PS) implant (Triathlon® series, Stryker®, Newbury, United Kingdom) as shown in Fig. 1. The position of the implant on the bone was verified by an experienced orthopaedic surgeon (the second author). It is important to note that a number of companies supply similar PS implants (e.g. Stryker: Triathlon™ series; DePuy: P.F.C. Sigma™ series; Smith & Nephew: Genesis II™ series) although minor details of the implant's external/internal geometry vary between manufactures. Finite element meshes for the intact and the implanted femurs were created and analysed in Abaqus 6.8.1 (Dassault Systemes, Simulia, Providence, RI, USA).

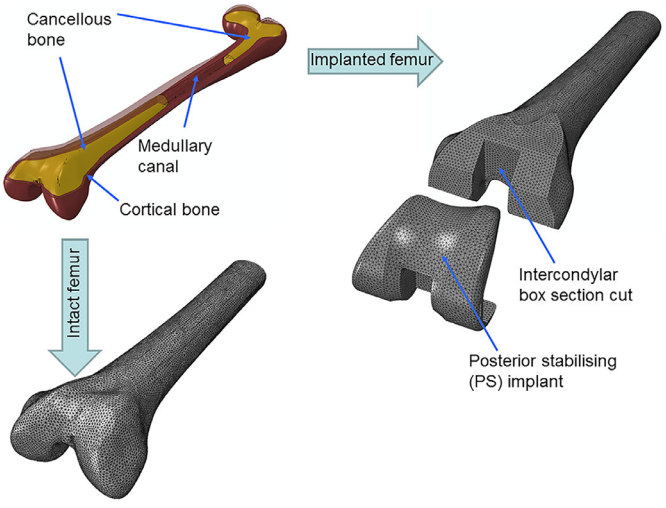

Fig. 1. Creation of intact and PS implanted distal femur FE meshes from CAD model of composite femur.

The meshes typically comprised of 290,000 10-noded tetrahedral elements. The average element size was 2 mm based on convergence studies (a further reduction in element size produced negligible change of displacements/stresses). Simulation runtime for each model was typically in the region of 2-3 hours, on a windows PC with a dual core i5 processor (2.6 GHz) and 8GB of ram.

2.1. Material properties

Cortical bone properties were based on whether healthy or pathological bone was being considered. Previous studies have shown that ageing results in cortical thinning [20,21] and a decrease in bone stiffness [24]. It has also been shown that with ageing, trabecularisation is initiated from the endosteum [20] resulting in the endosteum becoming much less stiff than the periosteum [24].

In this study, a heat transfer analysis was used as an artifice to assign variable elastic properties through the cortical thickness, e.g. from endosteum to periosteum. For this we took advantage of analysis capabilities available in Abaqus 6.8.1 used in this study. Indeed heat transfer capabilities are widely available in several FE packages. The first step was to assign a temperature of $\theta_1 = 0$ to the endosteal surface and a temperature of $\theta_2 = 1$ to the periosteal surface (Fig. 2a). A heat transfer analysis was then conducted with a unit value of thermal conductivity $k = 1\text{W/mm·K}$ and the temperatures were permitted to reach a steady state. The variation of temperatures through the cortical thickness is shown in Fig. 2a and b. These temperatures were then used as a proxy to assign variable elastic moduli to bone as a function of distance through the cortex, as shown in Fig. 2c, to create age dependent models. Before discussing these models it is important to emphasise that the variation of temperature so obtained (not the value itself) will not depend on the initial temperatures chosen (they only need to be different at the two surfaces) or the thermal conductivity. A similar technique was used by Davis et al. [25] to define regional inhomogeneity over complex biological structures.

In the current study, four relationships were then defined between Young's modulus (E) and temperature in order to characterise the inhomogeneity of bone properties (young and old) and to model cortical thinning as shown in Fig. 2c, as can be seen from the Figure, the periosteum always had a higher elastic modulus than the endosteum. Also the elastic moduli at the periosteum for old healthy (OH) and old osteoporotic (OOP) were assumed to be lower (16,700 MPa) than young healthy (YH) and young osteoporotic (YOP) bone (22,000 MPa).

Physically changing the geometry of the femur model to that of an osteoporotic geometry is not a trivial task due to its complex organic shape. Nevertheless, such changes are likely to be of significance to patient outcomes post-implantation. In this study, osteoporotic bone (both young and old) was characterised by a Young's modulus equivalent to that of cancellous bone (155 MPa) at the physical endosteum of the model, while the healthy endosteal value was offset to a spatial position representative of 50% of the cortical thickness (Fig. 2c mid-points on graph) using the aforementioned method for assigning a spatial distribution of properties to the bone. In this manner, the effect of cortical thinning was approximated through manipulation of stiffness values, acting as a proxy for geometrical changes which may occur due to osteoporosis and trabecularisation of the endosteum. Bousson et al. [20] showed that porosity increases more rapidly from periosteum to endosteum for older patients and Donaldson et al. [24] showed that for the femoral cortex porosity is linearly related to Young's modulus. The created models attempt to represent this. The Young's moduli at the endosteum were 16,700 MPa and 7000 MPa for YH and OH cases respectively. Values for both young and old bone material properties were based on values (average of

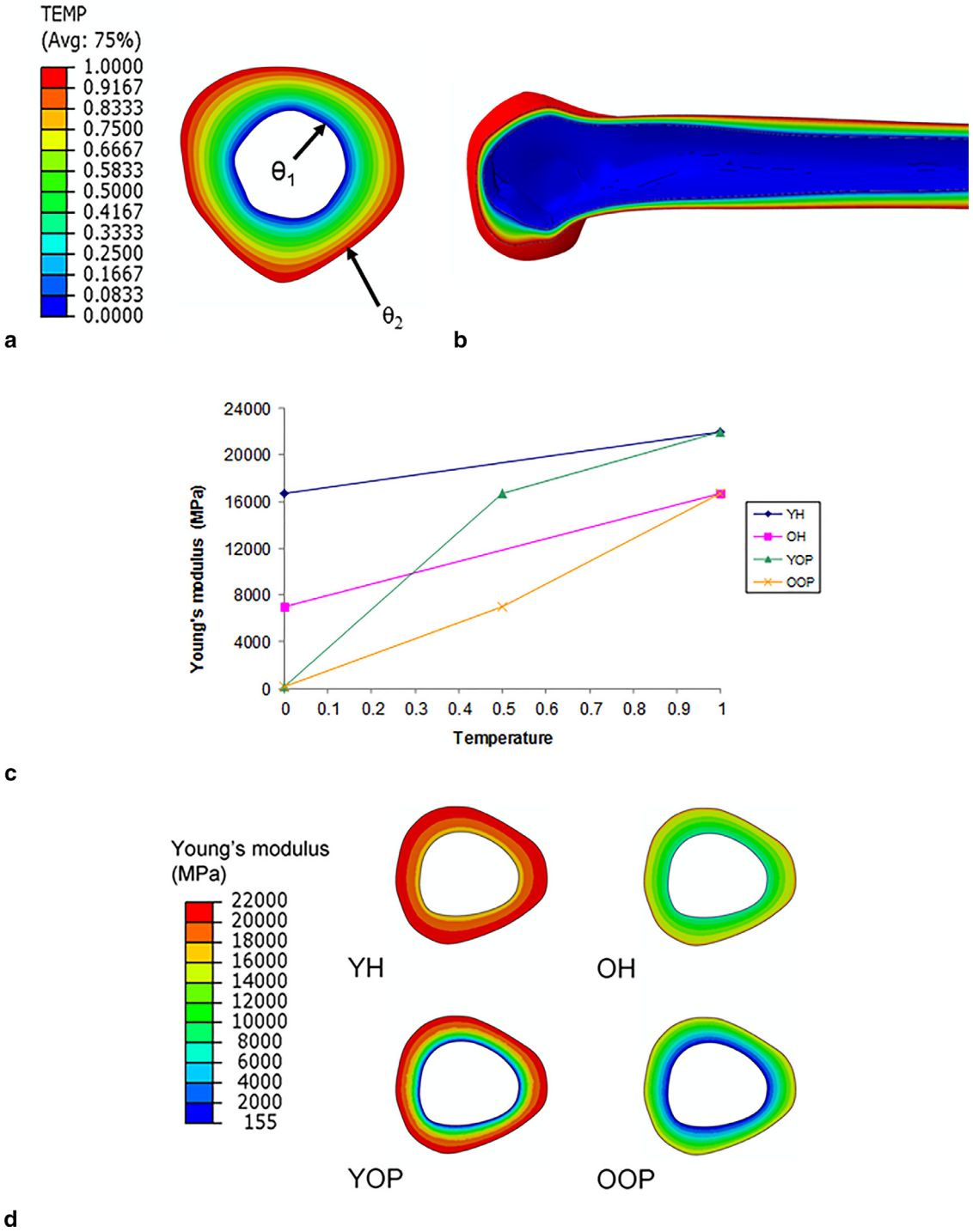

Fig. 2. (a) applied thermal boundary conditions, (b) resulting temperature gradient, (c) graph showing relationships between temperature and Young's modulus for each case investigated, and (d) cross section through the femur highlighting the distribution of Young's modulus following application of temperature methodology.

principal directions) taken from the literature [26]. The variation of elastic properties through cortical thickness for the four models created is shown in Fig. 2d. In all cases a Poisson's ratio = 0.3 was assumed for cortical bone regions.

All material property assignments were completed prior to any implantation. It is important to note that the method described above permits evaluation of the mechanical response due to age-related changes for essentially the same femur; this is not possible when employing CT based properties due to specimen specificity. The process also allows a simple method for assigning through thickness material properties which is not trivial, particularly if attempted manually. It is also important to point out that heat transfer analysis provides temperatures at the nodes, whereas material properties need to be assigned to integration points. This was achieved using element shape functions.

Application of inhomogeneous cortical bone properties to the femur pre- and post-implantation resulted in a total of eight different models (four intact and four implanted with the PS implant), each of these was examined under three different load cases (discussed below).

For all eight models, cancellous bone was assumed to be isotropic as in many previous studies, e.g. [20–22], with the values assigned to cancellous bone structures (Young's modulus = 155 MPa, Poisson's ratio = 0.3) being within the range of reported values from current literature [23,24]. Where relevant, the implant was assigned properties for a cobalt chromium alloy (E = 210,000 MPa, $\nu = 0.3$) in line with manufacturer's specifications (Stryker®, UK).

2.2. Boundary conditions

The choice of boundary conditions can greatly affect the output parameters being considered in an FE analysis (e.g. stresses, deformations), previous studies have shown that the stress distribution in the femur or pelvis can be altered significantly by the inclusion of boundary conditions that incorporate muscles and ligaments [27–29]. Studies within our group have also shown that the mechanical environment close to the points of load application is minimally affected by the restrained boundary conditions at some distance [19,27,30]. Therefore, the femur in this instance was fixed at a distance of 240 mm from the distal end. These boundary conditions are similar to most previous modelling studies [12–14,19,31,32]. Proximal fixation of the femur is also commonly employed in in vitro experiments examining knee implants e.g. [33,34].

2.3. Loading

There is large variability in reported loading of the knee joint for the same activity [35–47], as such this study considered forces acting on the knee as reported by previous studies that used in vivo telemetric implants [36,45]. To enable generation of consistent data sets load values were normalised in terms of subject body weight. This study considered three functional flexion angles (0°, 22°, and 48°) during the stance phase of gait for a normal walking cycle. Each flexion angle was modelled as a static load step. The load acting on the femur comprises of 6 separate components: patella-femoral force (PF); the medial and lateral components of the joint normal force (Fm and Fl); the medial and lateral components of the joint shear force (APm and APl); and the internal/external (IE) moment. The values used for the three flexion angles are given in Table 1. These forces were applied over realistic contact areas [48] as shown in Fig. 3, assuming correct alignment of the implant. Each of the six components of force were applied over three contact areas – PF, Fm and Fl acting normally and APm and APl tangentially on the corresponding contact areas for each of the flexion angles tested. Computationally the I/E moment was included by altering APm and APl forces.

Table 1
Forces used in the FE analyses for the three flexion angles. Values were obtained from previous in-vivo telemetric implant studies [36,45], normalised in terms of body weight and then applied to the FE model for an assumed average body weight of 775 N.

	0°	22°	48°
Medial Force Fm (N)	436	1159	1160
Lateral Force FL (N)	291	772	773
Medial Anterior–Posterior force APm (N)	−57	130	−3
Lateral Anterior–Posterior force APl (N)	−57	130	−3
Patella-Femoral Force PF (N)	45	327	567
Internal-External moment IE (Nmm)	−829	3292	−7029

2.4. Interface conditions

In all models incorporating the PS implant, the interface was modelled using tied constraints. These prohibit relative motions between the implant and bone at all contacting surfaces, simulating osseointegration of the implant into the host bone at the time of analysis.

3. Results

To highlight the overall impact of ageing and implantation on the mechanical environment in the distal femur post TKA, we first consider a frontal section c–c as shown in Fig. 4. We then examine

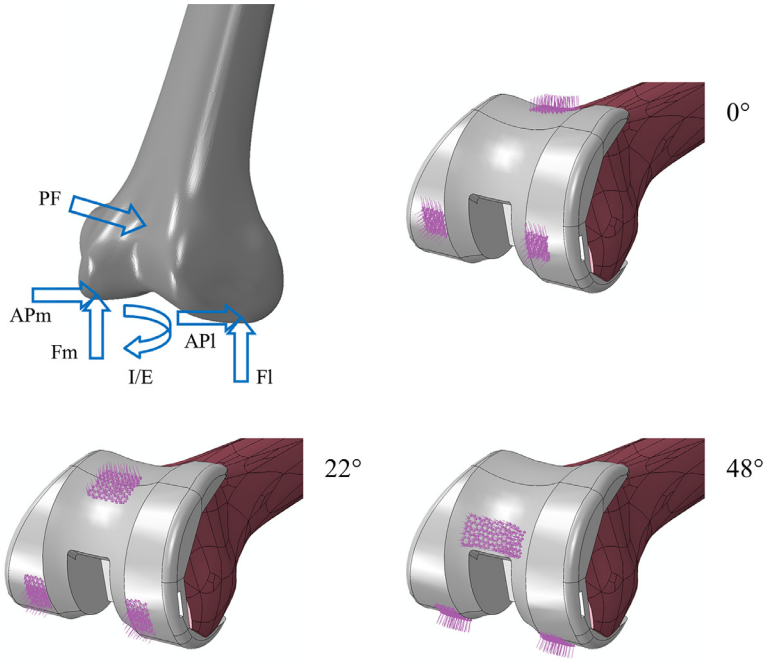

Fig. 3. Arrangement of forces acting on the knee joint (top-left), and regions over which they are applied for 0° (top-right), 22° (bottom-left) and 48° (bottom-right) flexion.

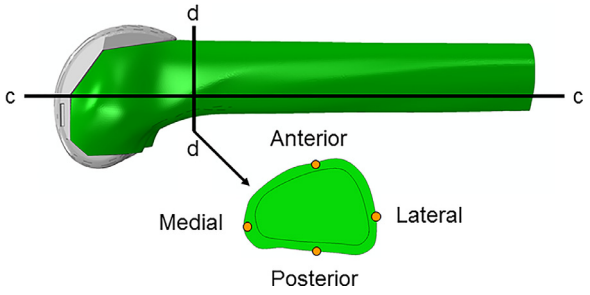

Fig. 4. Location of frontal (c–c) and transverse (d–d) sections taken through the femur. Also highlighted are four key points of interest on the cortex in the periprosthetic region at the location of section d–d.

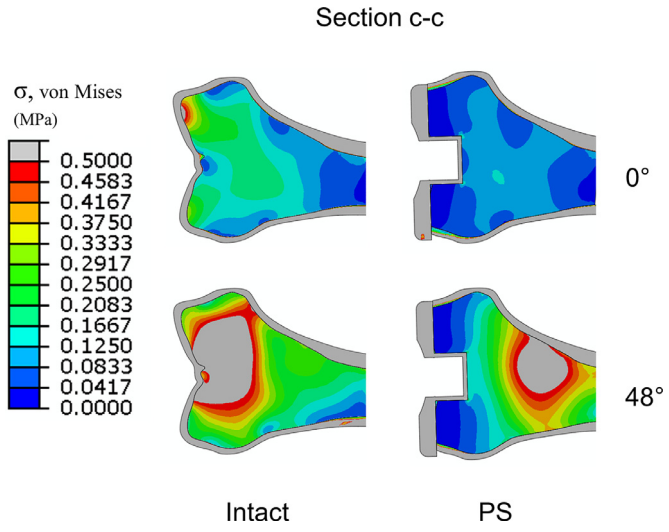

Fig. 5. Contour plot showing the magnitude and distribution of von Mises stress in the distal femur at section c–c, for both pre- and post-implantation scenarios, for the OOP case, at 0° and 48° flexion.

a transverse section (d–d) just above the implant, this region (d–d) has been shown to be critical with regard to fractures for both pre- and post-implantation cases [49–51]. For quantitative investigations, we also considered four representative points along the cortex at section d–d, as shown in Fig. 4.

Stress contours for both the intact and implanted (OOP cases) at section c-c are shown in Fig. 5. These show that post-implantation, large stresses shift proximally from the condylar region to the diaphyseal region, indicating stress-shielding in close proximity to the implant. This is possibly as a result of the concentrated joint force being distributed over a wider area due to the significant stiffness of the implant. It should also be noted that much larger stresses are generated at 48° flexion in comparison to 0° flexion. Stress contours at section d–d, once again for the OOP case, are shown in Fig. 6. While at the flexion angle of 0° the cortical stresses in the intact and implanted femurs are found to be almost identical, there is a significant difference at 48° flexion. Interestingly, at the higher flexion angles large cortical stresses are more widespread post-implantation (particularly in the anterior region).

Equivalent strains were examined for all four patient scenario investigated (YH, OH, YOP, OOP), for the 48° flexion angle as shown in Fig. 7. These show, that for all patient scenarios, strains at section c-c are significantly higher following implantation. The Figure also shows that old osteoporotic implanted bone experiences much larger strains in this region in comparison to young healthy bone.

In order to gauge the quantitative variations, von Mises stresses and equivalent strains were evaluated at the four representative points shown previously in Fig. 4, for all four patient scenarios and

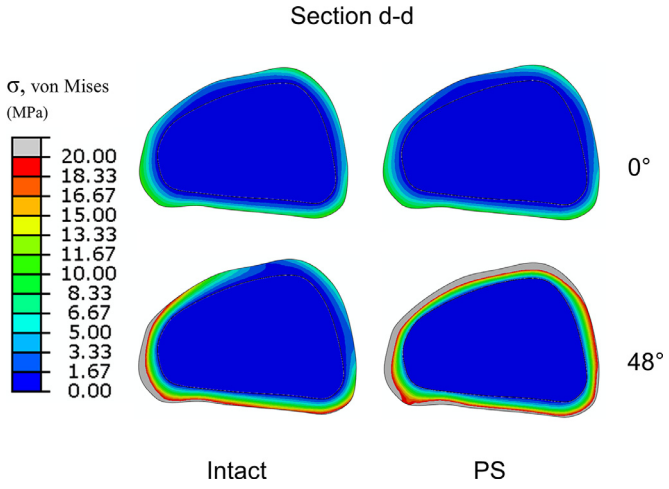

Fig. 6. Contour plot showing the magnitude and distribution of von Mises stress in the distal femur at section d–d, for both pre- and post-implantation scenarios, for the OOP case, at 0° and 48° flexion.

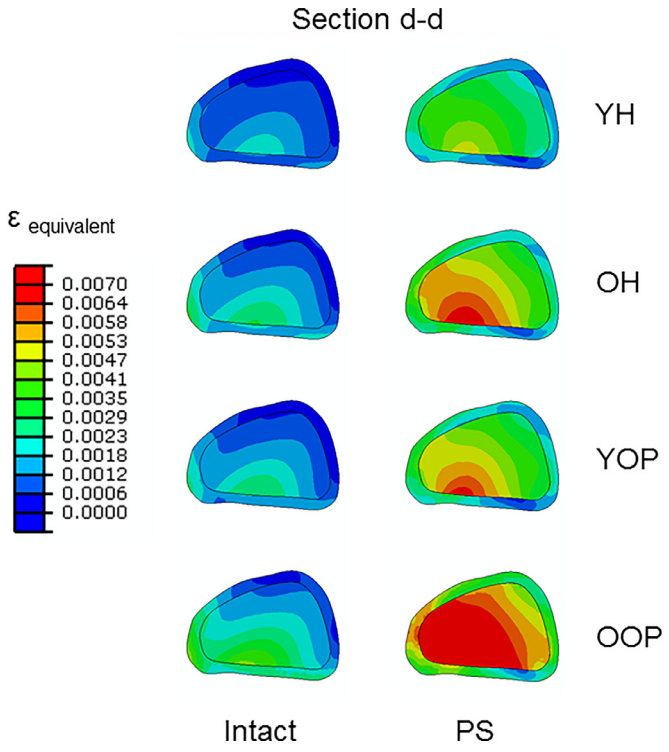

Fig. 7. Contour plots of the equivalent strain in the transverse section d–d for all cases at 48° flexion.

at each flexion angle investigated. The resulting values are presented in Figs. 8 and 9. At 0° flexion, stresses and strains at the four points considered are quite similar pre- and post-implantation (Fig. 8a and Fig. 9a), in fact stresses and strains are slightly higher for the intact case. This scenario changes completely with increasing flexion angle.

At 48° flexion, the stresses and strains are much higher post-implantation for all four points considered in comparison to the corresponding intact case (Fig. 8c and Fig. 9c). In all cases the OOP patients experience the largest strains and stresses, whereas the YH patients experiences the least, in general going from the YH case to OOP case lead to an approximate increase in stress of 68%. It is interesting to note, that at 0° flexion the stresses at the anterior location are very similar for both the intact and implanted

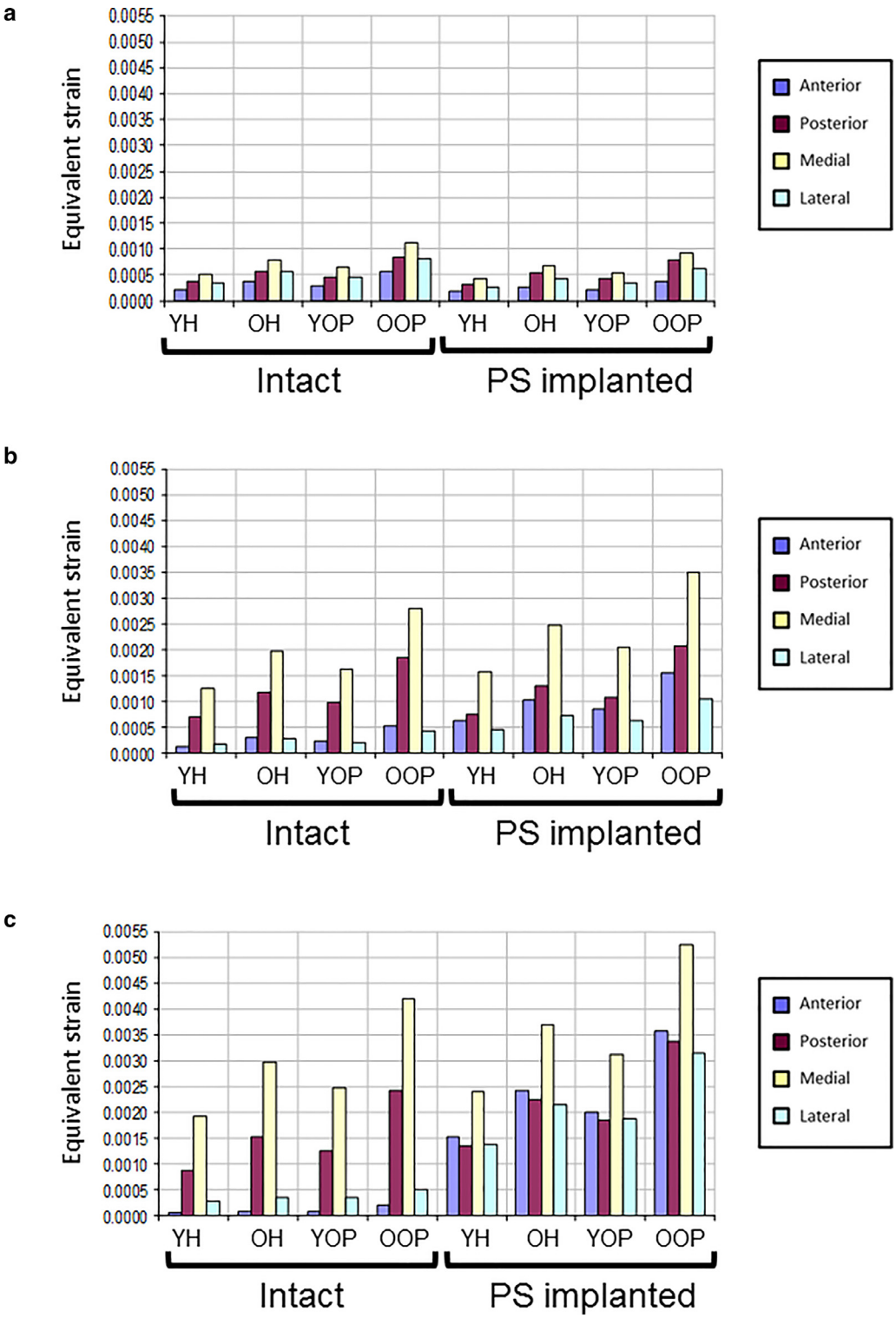

Fig. 8. Bar charts of equivalent strain at each of the four points of interest (indicated in Fig. 4) for all the cases investigated at (a) 0°, (b) 22°, and (c) 48° flexion.

cases. However, at higher flexion angles, the anterior stresses increase far more dramatically in the implanted cases, than at any other location. For example, if we examine the anterior point of interest for the OOP case, going from 0° to 48° flexion leads to an increase in von Mises stress from 4.17 MPa to 37.49 MPa for the implanted femur. However, stresses in the intact case are observed to decrease over the same flexion range, from 5.5 MPa at 0° flexion to 2.52 MPa at 48° flexion.

4. Discussion

The purpose of this study was to introduce a novel yet simple method to investigate the influence of ageing and osteoporosis on the mechanical environment in the femur pre- and post-implantation with a posterior stabilising (PS) femoral component. Multiple ageing and osteoporotic scenarios were modelled by employing this method on a single base femoral geometry.

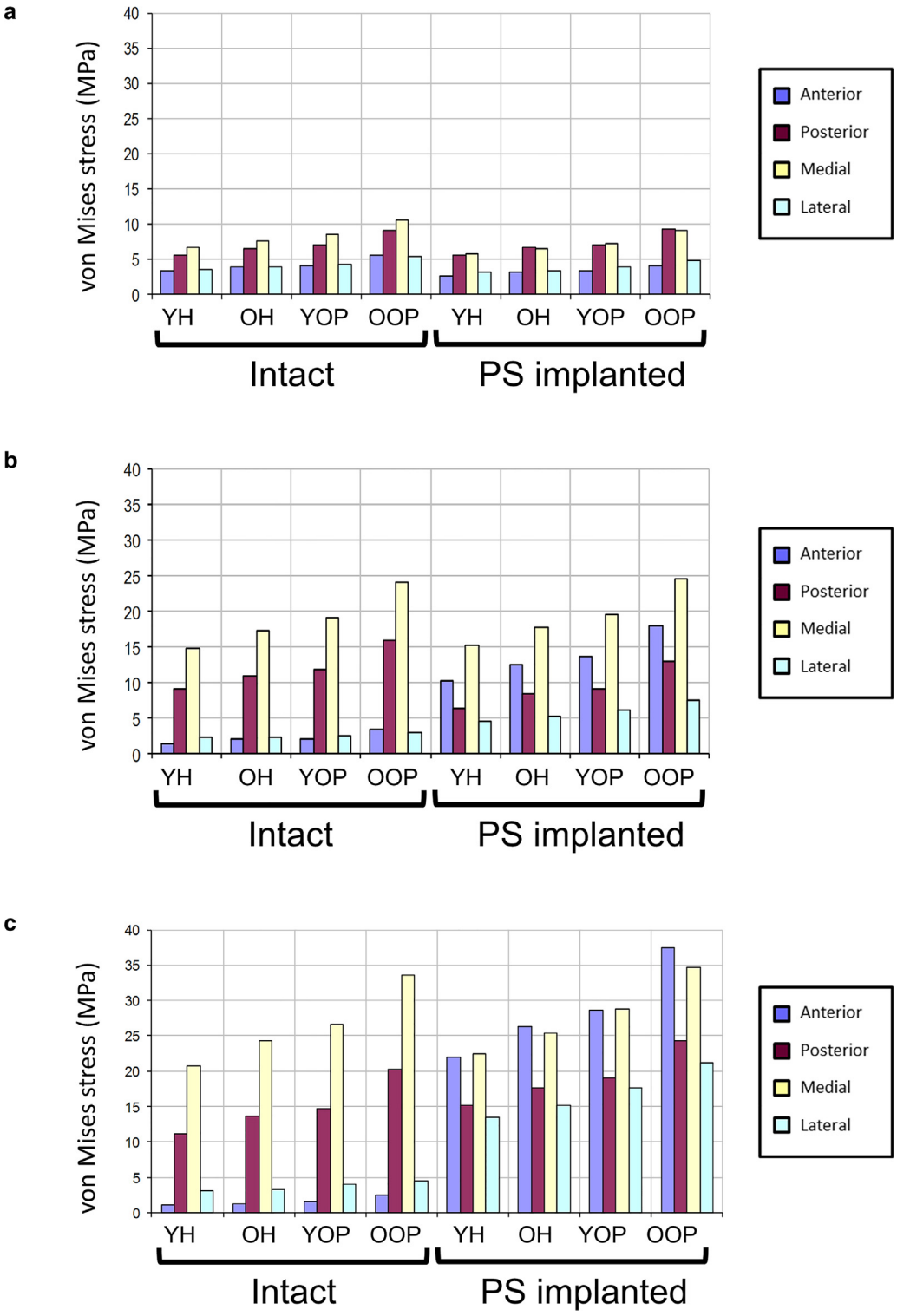

Fig. 9. Bar charts of von Mises stress at each of the four points of interest (indicated in Fig. 4) for all the cases investigated at (a) 0°, (b) 22°, and (c) 48° flexion.

Some studies [12–14], including those from our group [52], have incorporated variation of properties on the basis of CT attenuations from a specific patient/bone. A study by Au et al. [53] examined the effect of inhomogeneity using such a method, in the context of the intact distal femur and proximal tibia. However, these approaches and consequent results are subject-specific, and therefore cannot be used to establish general trends about a particular patient group. To our knowledge the comparative effect of inhomogeneity, moving from a young healthy to old osteoporotic scenario, on both the intact and implanted distal femur has not been previously examined. Furthermore, the authors are not aware of a comprehensive CT dataset containing multiple scans from the same subject at different ages/stages of disease progression that would permit this using a CT attenuation based approach. As such, this study has based the variations of Young's modulus values (from endosteum to periosteum) on the average of directional

values [26] obtained from a population specimen study. The level of cortical thinning was also based on data from population studies [20,21]. This approach permits us to evaluate such trends in the absence of subject specific data.

In this study, a virtual reconstruction [23] of the large left fourth generation composite femur (Sawbones, USA) was used as the base geometry for all models. By using a normalised bone geometry and applying the same loading and boundary conditions, (and in fact using the exact same mesh) we can say with some certainty that the observed differences in implant performance, e.g. under young healthy and old osteoporotic conditions, are as a direct result of changes to the material properties alone. This would not be so easy to discern should two different CT based patient-specific femurs (e.g. healthy and osteoporotic) be compared directly, as changes in shaft angulation, condylar shape/size, femoral alignment, and cortical thickness could obscure important trends.

As in several previous studies [9,10,13,14], our study shows that there is considerable stress-shielding distally under the femoral component, particularly in the condylar region [8,9] (as seen in Fig. 5). This fact has been well known. However, more importantly this study shows that the presence of an implant results in large stresses being transferred to the proximal region. This is much more pronounced at a higher flexion angle. This is apparently because at higher flexion angles loading is more likely to cause bending. For the implanted case stresses and strains shift proximally, generating higher stresses in the diaphysis, while the implant and the bone within it rotate as a rigid body in the distal region. This may also explain why periprosthetic fractures after total knee arthroplasty are often seen in the region just proximal to the femoral component. Further examination of these models also revealed that large stresses occur beyond the anterior flange post-implantation in the region widely associated with periprosthetic supracondylar fracture initiation [50,51]. Some previous studies have assessed the mechanical environment of the femur, or implant stability at 0° flexion e.g. [33,54]. In this study, as in previous work by the authors [19,34], it has been shown that consideration of higher flexion angles is critical when evaluating the performance of implants. Contrary to previously reported findings e.g. [55] 0° flexion is found to be inadequate for discerning key differences between femora, in particular with regard to stress-shielding.

Frequently in biomechanical studies it is stresses rather than strains that are examined and reported. Due to the low Young's modulus associated with cancellous bone regions, large stresses are rarely observed where there is cortical bone present to carry loads. However, in the present study a dramatic increase in the trabecular strains was observed due to ageing and osteoporosis post-implantation (as seen in Fig. 7). Similar findings were reported by van Rietbergen et al. [15] in the context of the proximal femur. In their study, μFE models of the femur were modified through manipulation of CT threshold values for trabecular bone to replicate osteoporotic microstructure. van Rietbergen et al. found that strains in the osteoporotic femur were much higher (by approximately 60%), with a less favourable and more widespread distribution.

In the present study, through incorporation of realistic loading conditions and more physiological material distributions through the cortex, it has been shown that both ageing and trabecularisation exert a significant effect on periprosthetic strain in the cortex of the intact and implanted femurs. It is important to recognise that any deterioration in material properties in the form of a reduced elastic modulus will result in an increase in strain. This is particularly evident in the OOP case, which incorporates both a reduction in properties and an element of thinning, and is found to exhibit the most significant rise in both strains and stresses. Interestingly we found that thinning itself (YOP) had a more significant impact on the mechanical environment of the femur than a simple reduction in stiffness (OH). This is likely due to the similar forces being transmitted over a reduced load bearing region due to trabecularisation of the endosteum. Previous studies on the effects of cortical thinning in the distal femur are limited. In a combined numerical and experimental study Zdero et al. [17] investigated how varying the thickness of the cortex impacted upon the response of the femur under mechanical testing conditions. Contrary to the present study, Zdero et al. concluded that only large amounts of bone loss in the cortical region would lead to a dramatic change in stiffness, and that the normal effects of aging would have less impact on its mechanical properties. A study by Anderson [56] investigated the effects of age related differences in joint torques and strain of the proximal femur during gait. It was concluded by the author that age did not significantly influence the likelihood of femoral fracture. However, as with the studies conducted by Zdero et al. changes to the material properties of the femur between young and old scenarios were not considered. Furthermore, in the case of Zdero et al. physiological loading at the knee joint was not replicated.

4.1. Limitations

In the present study cancellous and cortical bone stresses and strains were found to increase with age and thinning of the cortex. It is important to note that in situations where material properties degrade over time it is likely that both cancellous and cortical bone regions are simultaneously affected e.g. [57]. If changes to the cancellous bone structure were also considered this may result in an even greater proportion of load being carried across the thinned cortex increasing the potential risk of fracture even further.

In this study, a medial-lateral load distribution of 60–40% was assumed. This obviously results in a larger stress and strain being observed in the medial region. This would clearly change if the load distribution were modified, e.g. if incorporating malalignment due to disease. However, changes to the medial-lateral joint alignment are unlikely to influence the dramatic increase in anterior stress and strain observed in this study due to implantation. Another consideration is that the same magnitude of loading was considered for young and older patient scenarios, while this assumption permitted the direct comparison of the influence of age and thinning it may not be fully reflective of the in vivo situation where elderly patients may be more protective of their joints, particularly in the post-operative period following joint replacement and as a consequence may avoid full weight bearing on the operated limb for much longer than their younger counterparts.

We did not conduct any experimental validation of our simulations, which is a possible limitation. The complex loading experienced by the knee joint is not easy to replicate in a laboratory setting. Furthermore, incorporate of age related changes to bone properties in the lab would not be straightforward. Though the trends obtained in this study are likely to be valid; actual quantitative values may be different in an in vivo scenario where loading is dynamic and subject to external factors of the environment.

Finally, endosteal trabecularisation of the cortex is usually counteracted through apposition on the periosteal surface, particularly in male patients. The present study did not incorporate this feature and is therefore limited to modelling of female patients, who are known to suffer greater bone loss at the endosteal surface, with little to no apposition occurring at the periosteum [20,21]. As the initial response post-osseointegration was of interest in this study, this limitation was deemed acceptable. However, it is recognised that if the long term survival of the prosthesis is of interest (e.g. loosening or fracture), particularly in a male population where endosteal trabecularisation is less extreme and apposition plays an important role, then incorporation of a complex bone remodelling

framework, e.g. [58], would be required to more adequately capture the response of the femur to disease progression.

4.2. Clinical significance

Often an average case or limited number of patient specific cases is represented during testing and validation of new implant designs. However, this does not adequately account for the wide range of patients who may undergo TKA with the same prosthesis, and as such may not sufficiently represent all possible clinical scenarios. In the current study, the novel application of temperature dependent material properties as a means of modelling inhomogeneity and geometrical changes to the femur was found to be a powerful tool to allow rapid consideration of multiple clinical scenarios using the same base femoral geometry. Furthermore, use of this methodology allows for the incorporation of such changes independent of patient specific CT data, thereby limiting patient specific parameters from obscuring important trends and influencing results.

Ethical approval

Not required

Conflict of Interest

No conflict of Interest.

Acknowledgment

Support from the Lothian University Hospitals NHS Trust Brown and Ireland Estates Fund and The University of Edinburgh is gratefully acknowledged.

References

[1] NHS Scotland. Scottish arthroplasty project annual report. Information Services Division NHS Scotland. 2010.
[2] Font-Rodriguez DE, Scuderi GR, Insall JN. Survivorship of cemented total knee arthroplasty. Clin Orthopaed Relat Res 1997;345:79–86.
[3] Weir DJ, Moran CG, Pinder IM. Kinematic condylar total knee arthroplasty. J Bone Joint Surg, Br Vol 1996;78-B:907–11.
[4] Cadambi A, Engh GA, Dwyer KA, Vinh TN. Osteolysis of the distal femur after total knee arthroplasty. J Arthroplast 1994;9:579–94.
[5] Frosch P, Decking J, Theis C, Drees P, Schoellner C, Eckardt A. Complications after total knee arthroplasty: a comprehensive report. Acta Orthop Belg 2004;70:565–9.
[6] Meek RMD, Norwood T, Smith R, Brenkel IJ, Howie CR. The risk of peri-prosthetic fracture after primary and revision total hip and knee replacement. J Bone Joint Surg, Br Vol 2011;93-B:96–101.
[7] Petersen MM, Olsen C, Lauritzen JB, Lund B. Changes in bone mineral density of the distal femur following uncemented total knee arthroplasty. J Arthroplast 1995;10:7–11.
[8] Saari T, Uvehammer J, Carlsson LV, Regnér L, Kärrholm J. Posterior stabilized component increased femoral bone loss after total knee replacement. 5-year follow-up of 47 knees using dual energy X-ray absorptiometry. Knee 2006;13:435–9.
[9] Soininvaara TA, Miettinen HJA, Jurvelin JS, Suomalainen OT, Alhava EM, Kröger HPJ. Periprosthetic femoral bone loss after total knee arthroplasty: 1-year follow-up study of 69 patients. Knee 2004;11:297–302.
[10] Spittlehouse AJ, Getty CJ, Eastell R. Measurement of bone mineral density by dual-energy x-ray absorptiometry around an uncemented knee prosthesis. J Arthroplast 1999;14:957–63.
[11] Rayan F, Konan S, Haddad FS. A review of periprosthetic fractures around total knee arthroplasties. Curr Orthopaed 2008;22:52–61.
[12] Barink M, Verdonschot N, de Waal Malefijt M. A different fixation of the femoral component in total knee arthroplasty may lead to preservation of femoral bone stock. Proc Inst Mech Eng, Part H: J Eng Med 2003;217:325–32.
[13] van Lenthe GH, de Waal Malefijt MC, Huiskes R. Stress shielding after total knee replacement may cause bone resorption in the distal femur. J Bone Joint Surg Br Vol 1997;79-B:117–22.
[14] van Lenthe GH, Willems MMM, Verdonschot N, de Waal Malefijt MC, Huiskes R. Stemmed femoral knee prostheses: effects of prosthetic design and fixation on bone loss. Acta Orthopaed Scand 2002;73:630.
[15] van Rietbergen B, Huiskes R, Eckstein F, Rüegsegger P. Trabecular bone tissue strains in the healthy and osteoporotic human femur. J Bone Mineral Res 2003;18:1781–8.
[16] Verhulp E, van Rietbergen B, Huiskes R. Load distribution in the healthy and osteoporotic human proximal femur during a fall to the side. Bone 2008;42:30–5.
[17] Zdero R, Bougherara H, Dubov A, Shah S, Zalzal P, Mahfud A, et al. The effect of cortex thickness on intact femur biomechanics: a comparison of finite element analysis with synthetic femurs. Proc Inst Mech Eng, Part H: J Eng Med 2010;224:831–40.
[18] Brown TA, Kohan L, Ben-Nissan B. Assessment by finite element analysis of the impact of osteoporosis and osteoarthritis on hip resurfacing. In: Proceedings of the 5th Australasian Congress on Applied Mechanics. Brisbane, Austrailia; 2007.
[19] Conlisk N, Howie CR, Pankaj P. The role of complex clinical scenarios in the failure of modular components following revision total knee arthroplasty: a finite element study. J Orthopaed Res 2015;33:1134–41.
[20] Bousson V, Meunier A, Bergot C, É Vicaut, Rocha MA, Morais MH, et al. Distribution of intracortical porosity in human midfemoral cortex by age and gender. J Bone Mineral Res 2001;16:1308–17.
[21] Russo CR, Lauretani F, Seeman E, Bartali B, Bandinelli S, Di Iorio A, et al. Structural adaptations to bone loss in aging men and women. Bone 2006;38:112–18.
[22] Cooper DML, Thomas CDL, Clement JG, Turinsky AL, Sensen CW, Hallgrímsson B. Age-dependent change in the 3D structure of cortical porosity at the human femoral midshaft. Bone 2007;40:957–65.
[23] BEL Repository. 2008, http://www.biomedtown.org/biomed_town/LHDL/Reception/datarepository/repositories/BEL/repository/wh_view.
[24] Donaldson FE, Pankaj P, Cooper DML, Thomas CDL, Clement JG, Simpson AHRW. Relating age and micro-architecture with apparent-level elastic constants: a micro-finite element study of female cortical bone from the anterior femoral midshaft. Proc Inst Mech Eng, Part H: J Eng Med 2011;225:585–96.
[25] Davis JL, Dumont ER, Strait DS, Grosse IR. An efficient method of modeling material properties using a thermal diffusion analogy: an example based on craniofacial bone. PLoS One 2011;6:e17004.
[26] Donaldson FE, Pankaj P, Simpson AHRW. Investigation of factors affecting loosening of ilizarov ring-wire external fixator systems at the bone-wire interface. J Orthopaed Res 2012;30:726–32.
[27] Phillips ATM. The femur as a musculo-skeletal construct: a free boundary condition modelling approach. Med Eng Phys 2009;31:673–80.
[28] Phillips ATM, Pankaj P, Howie CR. Finite element modelling of the pelvis: inclusion of muscular and ligamentous boundary conditions. Med Eng Phys 2007;29:739–48.
[29] Speirs AD, Heller MO, Duda GN, Taylor WR. Physiologically based boundary conditions in finite element modelling. J Biomech 2007;40:2318–23.
[30] Kerr C, Wilkie Y, Conlisk N, Pankaj P, Howie CR. How Sophisticated does a Model need to be to capture the mechanical environment in the femur. In: Proceedings of the 23rd Congress of the International Society of Biomechanics. Brussels, Belgium; 2011.
[31] Completo A, Simões JA, Fonseca F. Revision total knee arthroplasty: the influence of femoral stems in load sharing and stability. Knee 2009;16:275–9.
[32] Tissakht M, Ahmed AM, Chan KC. Calculated stress-shielding in the distal femur after total knee replacement corresponds to the reported location of bone loss. J Orthopaed Res 1996;14:778–85.
[33] Completo A, Fonseca F, Simões JA. Experimental validation of intact and implanted distal femur finite element models. J Biomech 2007;40:2467–76.
[34] Conlisk N, Gray H, Pankaj P, Howie CR. The influence of stem length and fixation on initial femoral component stability in revision total knee replacement. Bone Joint Res 2012;1:281–8.
[35] Andriacchi TP, Andersson GBJ, Fermier RW, Stern D, Galante JO. A study of lower-limb mechanics during stair-climbing. J Bone Joint Surg 1980;62:749–57.
[36] Bergmann G. 2008, http://www.OrthoLoad.com.
[37] Dahlkvist NJ, Mayo P, Seedhom BB. Forces during squatting and rising from a deep squat. Eng Med 1982;11:69–76.
[38] D'Lima DD, Patil S, Steklov N, Slamin JE, Colwell Jr CW. Tibial forces measured in vivo after total knee arthroplasty. J Arthroplast 2006;21:255–62.
[39] Ellis MI, Seedhom BB, Wright V. Forces in the knee joint whilst rising from a seated position. J Biomed Eng 1984;6:113–20.
[40] Fregly BJ, Besier TF, Lloyd DG, Delp SL, Banks SA, Pandy MG, et al. Grand challenge competition to predict in vivo knee loads. J Orthopaed Res 2012;30:503–13.
[41] Heinlein B, Kutzner I, Graichen F, Bender A, Rohlmann A, Halder AM, et al. ESB clinical biomechanics award 2008: complete data of total knee replacement loading for level walking and stair climbing measured in vivo with a follow-up of 6–10 months. Clin Biomech 2009;24:315–26.
[42] Kuster MS, Wood GA, Stachowiak GW, Gächter A. Joint load considerations in total knee replacement. J Bone Joint Surg, Br Vol 1997;79-B:109–13.
[43] Morrison JB. The mechanics of the knee joint in relation to normal walking. J Biomech 1970;3:51–61.
[44] Taylor SJG, Walker PS. Forces and moments telemetered from two distal femoral replacements during various activities. J Biomech 2001;34:839–48.
[45] Taylor SJG, Walker PS, Perry JS, Cannon SR, Woledge R. The forces in the distal femur and the knee during walking and other activities measured by telemetry. J Arthroplast 1998;13:428–37.

[46] Taylor WR, Heller MO, Bergmann G, Duda GN. Tibio-femoral loading during human gait and stair climbing. J Orthopaed Res 2004;22:625–32.
[47] Thambyah A. How critical are the tibiofemoral joint reaction forces during frequent squatting in Asian populations? Knee 2008;15:286–94.
[48] Goudakos IG, König C, Schöttle PB, Taylor WR, Hoffmann J-E, Pöpplau BM, et al. Regulation of the patellofemoral contact area: an essential mechanism in patellofemoral joint mechanics. J Biomech 2010;43:3237–9.
[49] Distal Femur AAOS. (Thighbone) fractures of the knee. American Academy of Orthopaedic Surgeons; 2010.
[50] Dennis DA. Periprosthetic fractures following total knee arthroplasty. J Bone Joint Surg 2001;83:120.
[51] Beris AE, Lykissas MG, Sioros V, Mavrodontidis AN, Korompilias AV. Femoral periprosthetic fracture in osteoporotic bone after a total knee replacement: treatment with ilizarov external fixation. J Arthroplast 2010;25:1168.e9–e12.
[52] Goffin JM, Pankaj P, Simpson AH. The importance of lag screw position for the stabilization of trochanteric fractures with a sliding hip screw: a subject-specific finite element study. J Orthopaed Res 2013;31:596–600.
[53] Au AG, Liggins AB, Raso VJ, Carey J, Amirfazli A. Representation of bone heterogeneity in subject-specific finite element models for knee. Comput Methods Programs Biomed 2010;99:154–71.
[54] Bougherara H, Nazgooei S, Sayyidmousavi A, Maršık F, Mařík IA. Computation of bone remodelling after Duracon knee arthroplasty using a thermodynamic-based model. Proc Inst Mech Eng, Part H: J Eng Med 2011;225:669–79.
[55] Bougherara H, Zdero R, Mahboob Z, Dubov A, Shah S, Schemitsch EH. The biomechanics of a validated finite element model of stress shielding in a novel hybrid total knee replacement. Proc Inst Mech Eng Part H-J Eng Med 2010;224:1209–19.
[56] Anderson DE. An examination of age-related differences in lower extremity joint torques and strains in the proximal femur during gai. Virginia Polytechnic Institute and State University; 2010.
[57] Milovanovic P, Potocnik J, Djonic D, Nikolic S, Zivkovic V, Djuric M, et al. Age-related deterioration in trabecular bone mechanical properties at material level: nanoindentation study of the femoral neck in women by using AFM. Exp Gerontol 2012;47:154–9.
[58] Ruimerman R, Hilbers P, van Rietbergen B, Huiskes R. A theoretical framework for strain-related trabecular bone maintenance and adaptation. J Biomech 2005;38:931–41.